

This article was downloaded by:

On: 14 January 2011

Access details: *Access Details: Free Access*

Publisher *Taylor & Francis*

Informa Ltd Registered in England and Wales Registered Number: 1072954 Registered office: Mortimer House, 37-41 Mortimer Street, London W1T 3JH, UK



## Molecular Simulation

Publication details, including instructions for authors and subscription information:

<http://www.informaworld.com/smpp/title~content=t713644482>

### A novel hybrid simulation for study of multiscale phenomena

P. E. Krouskop<sup>a</sup>; J. Garrison<sup>a</sup>; P. C. Gedeon<sup>a</sup>; J. D. Madura<sup>a</sup>

<sup>a</sup> Department of Chemistry and Biochemistry, Duquesne University, Pittsburgh, PA, USA

**To cite this Article** Krouskop, P. E. , Garrison, J. , Gedeon, P. C. and Madura, J. D.(2006) 'A novel hybrid simulation for study of multiscale phenomena', *Molecular Simulation*, 32: 10, 825 — 830

**To link to this Article:** DOI: 10.1080/08927020600779368

**URL:** <http://dx.doi.org/10.1080/08927020600779368>

PLEASE SCROLL DOWN FOR ARTICLE

Full terms and conditions of use: <http://www.informaworld.com/terms-and-conditions-of-access.pdf>

This article may be used for research, teaching and private study purposes. Any substantial or systematic reproduction, re-distribution, re-selling, loan or sub-licensing, systematic supply or distribution in any form to anyone is expressly forbidden.

The publisher does not give any warranty express or implied or make any representation that the contents will be complete or accurate or up to date. The accuracy of any instructions, formulae and drug doses should be independently verified with primary sources. The publisher shall not be liable for any loss, actions, claims, proceedings, demand or costs or damages whatsoever or howsoever caused arising directly or indirectly in connection with or arising out of the use of this material.

# A novel hybrid simulation for study of multiscale phenomena

P. E. KROUSKOP\*, J. GARRISON, P. C. GEDEON and J. D. MADURA

Department of Chemistry and Biochemistry, Duquesne University, 600 Forbes Ave., Pittsburgh, PA 15282, USA

(Received January 2006; in final form May 2006)

A novel multiscale model and simulation has been developed by combining the algorithms from a course grained 2D lattice model with Brownian dynamics (BD). The lattice model incorporates Lennard-Jones and coulombic interactions between particles, as well as nearest-neighbor interactions. The BD simulation allows the particles to move in solution before they adsorb to the surface. This hybrid simulation is used to study the behavior of nanoparticles in the presence of a surface and evaporation of solvent. The simulation is able to produce amorphous topologies of nanoparticles on the surface.

**Keywords:** Multiscale; Quantum dots; Brownian dynamics; Lattice model

## 1. Introduction

One of the proposed uses of nanotechnology is in the study and treatment of disease in biology. Potential areas of application are in biological imaging [1–3], drug delivery [4], and as biosensors [5–8]. To enhance the engineering of devices to be used in these applications, a fundamental understanding of nanoscale device interaction with proteins and biological surfaces is necessary. This understanding can be achieved through the use of existing computer models and the development of novel algorithms in cooperation with experiment.

Currently, materials scientists are examining the interaction of nanoparticles with surfaces in the development of novel materials and devices. One interesting phenomenon that has been observed in nanoscale device construction is the formation of mesoscopic patterns consisting of groups of nanoparticles. The patterns that are formed have been found to be dependent upon the shape of the nanoparticle, evaporation rate of the solvent, as well as the nature of the substrate. Sau and Murphy [9] have observed that mesoscopic patterns are formed from gold nanorods and nanospheres. They showed that the patterns were dependent on the shape of the nanoparticles, and on the functionality of the surfactant used. Vysotskii *et al.* [10] showed that the evaporation rate of the solvent affected the patterns formed by silver nanoparticles. They were able to obtain two-dimensional (2D) and three-dimensional (3D) fractal structures depending on

the evaporation rate and nature of the substrate. In the development of optoelectronic devices, Pagan *et al.* have observed circular rings of CdSe forming during the spin-casting fabrication process [11]. Coe-Sullivan and co-workers have devised a phase separation process to obtain ordered monolayers of nanoparticles on surfaces [12]. They show that the properties of the resulting films are dependent on the quantum dot size distribution, morphology, and concentration in solution.

Several researchers have developed models and simulations to study the aggregation process in various systems [13–20]. Jarai-Szabo and co-workers have developed a computer simulation technique based on a “spring-block stick-slip model” to compare to 2D, self-assembled structures obtained experimentally from drying a colloidal suspension of nanoparticles on a surface [21]. Their computer model qualitatively reproduces the observed patterns, and the investigators have derived the dynamics of the process based on their model. Another computer model, based on a 2D grid, has also been developed and used by Rabani *et al.* to study the patterns formed as a nanoparticle solution is dried on a surface [22]. This computer model has recently been extended to three dimensions, and the formation of “stalagmite” type structures has been observed [23]. McCabe and co-workers have developed a multiscale simulation to investigate the self-assembly of polyhedral oligomeric silsesquioxane molecules into networks [24]. Their multiscale approach covers electronic, atomistic and mesoscale distances.

\*Corresponding author. Email: krouskop@duq.edu

In this work, we will present proof of concept results for a multiscale simulation. The simulation combines a Brownian dynamics (BD) simulation technique with the 2D, lattice model of Rabani and co-workers [22]. This allows the continuum of the solvent to be modeled more realistically than the grid used by Sztrum and co-workers [23]. The new model will allow the quantum dots to diffuse to the surface, and the kinetics of the self-assembly process may be inferred.

## 2. Models and algorithms

In this paper we present results from modifications to the model reported by Rabani *et al.* [22]. We extend the previous model by adding coulombic and Lennard-Jones (LJ) potentials. We also append a BD algorithm to form a hybrid BD/course-grained model.

### 2.1 2D-lattice model

We calculate the nearest-neighbor interaction energies for our system using the same energy calculation presented in previous work [22]:

$$H = -\epsilon_l \sum_{\langle ij \rangle} l_i l_j - \epsilon_n \sum_{\langle ij \rangle} n_i n_j - \epsilon_{nl} \sum_{\langle ij \rangle} n_i l_j - \mu \sum_i l_i. \quad (1)$$

The first three summations determine the energies for solvent-solvent, particle-particle, and particle-solvent interactions respectively, and the last sum allows the solvent to evaporate. The values for  $\epsilon_l$ ,  $\epsilon_n$ ,  $\epsilon_{nl}$ , which determine the magnitude of the interaction energies are set at  $2k_B T$ ,  $2\epsilon_l$  and  $1.5\epsilon_l$ , respectively, to match those used by Rabani *et al.* [22]. The value of the chemical potential is set at  $-2.25\epsilon_l$  to allow the solvent to dry at a reasonable rate. The sums over  $\langle ij \rangle$  are over the nearest-neighbor cells  $j$  that share a side with cell  $i$ . Thus, interactions along the diagonal are precluded and there are only four adjacent cells to any given cell on the grid.

We have extended this model to account for longer range interactions between the nanoparticles. We have included a LJ potential

$$H_{LJ} = \sum_{i < j} 4\epsilon_{LJ} \left[ \left( \frac{\sigma}{r_{ij}} \right)^{12} - \left( \frac{\sigma}{r_{ij}} \right)^6 \right], \quad (2)$$

where  $\epsilon_{LJ} = 4.5\epsilon_l$  and  $\sigma = 1.28 \times 10^{-8}$  m. The distance between nanoparticles  $i$  and  $j$  ( $r_{ij}$ ) is determined between each pair of nanoparticles in the system, not just nearest-neighbors. We have also added long-range Coulombic interactions using the Debye-Hückel model [25]

$$H_C = \frac{1}{4\pi\epsilon_0} \sum_{i < j} z_i z_j \left[ \frac{e^{\kappa d}}{1 + \kappa d} \frac{e^{-\kappa r_{ij}}}{r_{ij}} \right], \quad (3)$$

where  $z_i$  is the charge on particle  $i$ ,  $1/\kappa$  is the Debye length,  $d$  is the diameter of the particle, and  $r_{ij}$  is the distance between particles  $i$  and  $j$ . The nanoparticles are modeled

with a single charge per particle, or up to four charges per particle (one on each corner).

### 2.2 Brownian dynamics algorithm

We have also paired the 2D lattice algorithm with a 3D BD algorithm. We use this hybrid simulation to study the interactions of the nanoparticles as they come out of solution, and coalesce on the surface.

The BD are modeled using the Ermack-McCammon equation [26].

$$r(t + \delta t) = r(t) + \sum_{\langle ij \rangle} \frac{F_{ij} D_{ij}}{k_B T} \delta t + R \quad (4)$$

where  $F_{ij}$  is the force between particles  $i$  and  $j$ ,  $D_{ij}$  is the joint diffusion coefficient for particles  $i$  and  $j$ ,  $k_B$  is Boltzmann's constant,  $T$  is the temperature in Kelvin, and  $R$  is a randomly chosen displacement vector. The value of  $R$  is chosen from a Gaussian distribution with a zero mean and a variance of  $2D_{ij}\delta t$ . We have chosen a diffusion coefficient of  $5.0 \times 10^{-6} \text{ cm}^2/\text{s}$ . The  $F_{ij}$  are currently calculated using the LJ potential discussed above.

## 3. Results and discussion

To verify our interpretation of the work done by Rabani *et al.*, we simulated a system using the parameters presented in their paper. The results, shown in figure 1, qualitatively match the reported results for systems with nanoparticle density of  $\rho = 0.30$  (18,750 particles) on

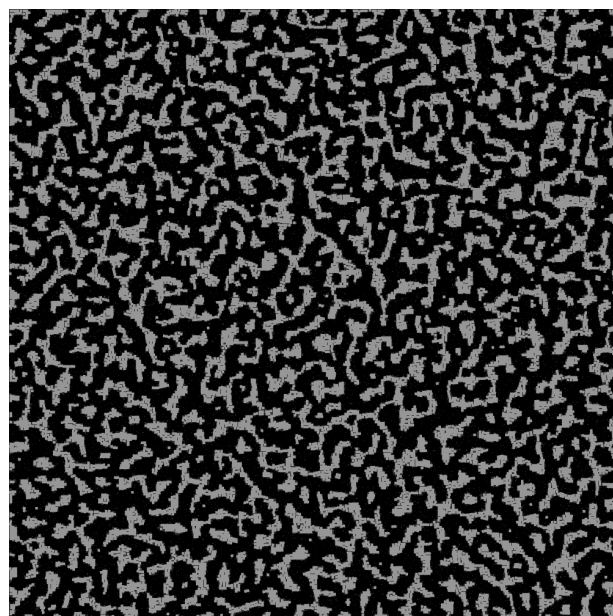


Figure 1. Results from  $150 \times 10^6$  Monte-Carlo steps of the 2D simulation. The black areas are bare surface, the gray areas are solvent, and the white areas are nanoparticles. The simulation parameters, taken from Ref. [22] are:  $\epsilon_l = 8.2842 \times 10^{-21}$ ,  $\epsilon_n = 1.65684 \times 10^{-20}$ ,  $\epsilon_{nl} = 1.24263 \times 10^{-20}$  and  $\mu = -1.863945 \times 10^{-20}$  which correspond to a temperature of 300 K.

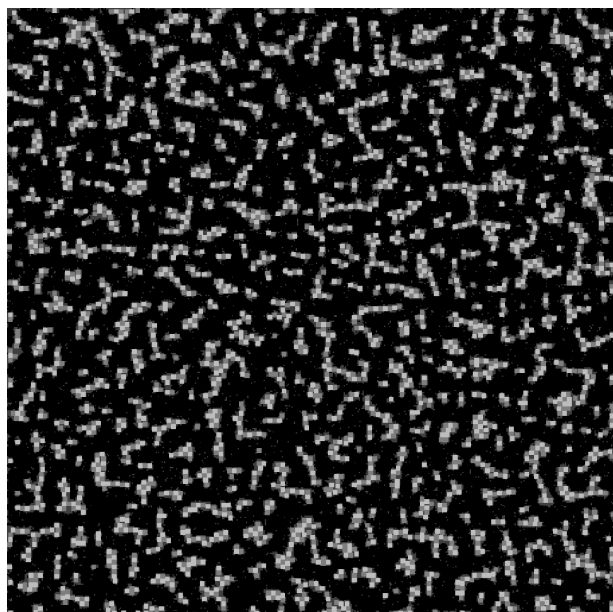


Figure 2. Results from  $3 \times 10^6$  Monte-Carlo steps of the 2D simulation with Coulombic interactions. The black areas are dry, the dark squares are negative charges, and the light squares are positive charges. The simulation parameters are:  $\epsilon_f = 8.2842 \times 10^{-21}$  J,  $\epsilon_n = 1.65684 \times 10^{-20}$  J,  $\epsilon_{nl} = 1.24263 \times 10^{-20}$  J,  $\mu = -1.863945 \times 10^{-20}$  J and  $\kappa = 1.00 \times 10^7$  m.

a grid of 1000 by 1000 cells. The nanoparticles are given a diameter of four lattice cells, and each lattice cell is given a dimension of 1.0 nm on a side. The results show amorphous aggregation of the nanoparticles as the solvent dries. Note that the particles form dense regions with a very tortuous topology. This is very different from the precise rings and patterns that have been experimentally observed [9,11,12], indicating that these precise topologies are not controlled by nearest-neighbor interactions alone.

### 3.1 Nanoparticles with electrostatic interactions

We have extended the system to include charged nanoparticles. The first study consisted of a mixture of positive and negative charged particles. The results from a system with a total nanoparticle density of  $\rho = 2.0 \times 10^{-2}$  (327 particles) on a 512 by 512 grid is shown in figure 2. The nanoparticles are observed to quickly group, and then not move much once groups of four or more are established. This results from the Coulombic attraction, and the model moving one nanoparticle at a time. The probability of moving away from an oppositely charged particle at the simulated temperature is small. If groups were moved instead of single particles, we would expect to observe larger aggregates.

The nanoparticles were also simulated with multiple charges per particle. When each particle has a positive charge in one corner and a negative charge in the opposite corner, simulating a dipole, the system evolves in a manner similar to that seen above (figure 3). The aggregates,

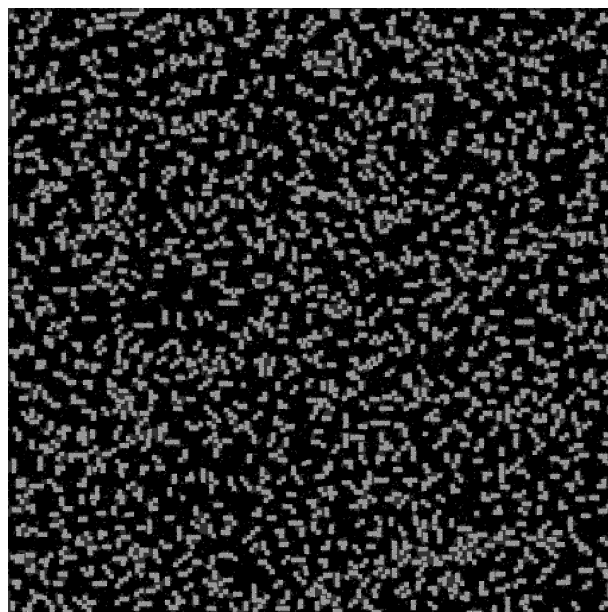


Figure 3. Results from  $3 \times 10^6$  Monte-Carlo steps of the 2D simulation with Coulombic interactions on a  $512 \times 512$  grid. The charges on the nanoparticles are placed on opposite corners. The black areas are dry. The simulation parameters are the same as those presented in figure 2.

however, appear to be composed of fewer nanoparticles, creating more groups that are smaller in size than observed above. There are also diagonal lines that form as the positive and negative charges attract each other. The diagonal lines remain small since the nanoparticle interactions (those calculated using  $\epsilon_n$ ) are not calculated on the diagonal, and the nanoparticles are able to move, unlike the pairs of nanoparticles observed in the mixture of positive and negative charges above. The greater freedom to move keeps the groups small.

### 3.2 Nanoparticles with Lennard-Jones and electrostatic interactions

Systems of charged, LJ particles were also simulated. The simulation parameters for these systems are a grid that is 512 by 512 with  $\rho = 2.0 \times 10^{-2}$  (327 particles),  $\mu = -1.65684 \times 10^{-20}$  J, and  $\sigma = 1.28 \times 10^{-8}$  m.

In figure 4, the particles all carry the same charge, which would result in all the particles repelling each other except for the LJ terms. It can be seen that the LJ interactions create loose aggregates of the particles. In figure 5, the particles carry either a positive or negative charge. The particles now group together with alternating charges, as expected, but the tight groups observed in figure 3 are not possible due to the LJ repulsion. Because the particles never come into direct contact, the  $\epsilon_n$  term of the energy calculation does not contribute anything. Further investigation of the effects of  $\sigma$  and  $\epsilon_{LJ}$  are warranted to determine how the long-range electrostatic and LJ potentials interact with the particle-particle interactions to form mesoscale structures on the surface.



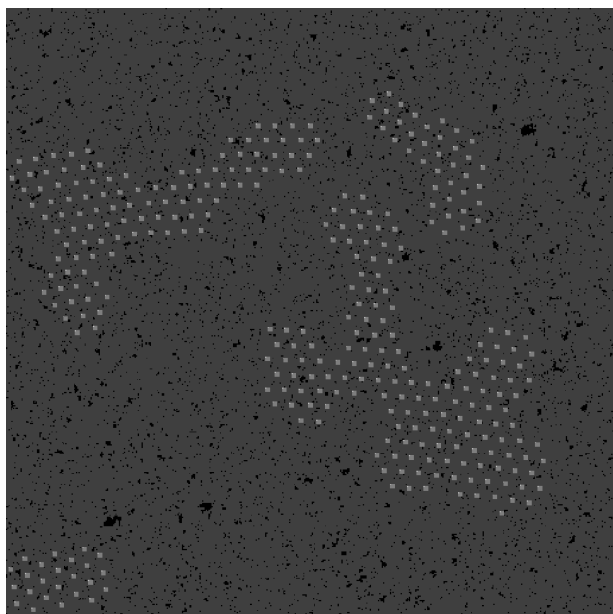


Figure 4. Results from  $150 \times 10^7$  Monte-Carlo steps of the 2D simulation of same-charged nanoparticles with LJ interactions on a  $512 \times 512$  grid. The simulation parameters are:  $\epsilon_{LJ} = 3.72789 \times 10^{-20}$  J, and  $\kappa = 1.00 \times 10^8$  m. All other parameters not defined in the text are the same as in figure 2.

### 3.3 Hybrid BD/lattice simulation

We have developed a hybrid simulation consisting of BD and the 2D, course-grained simulation discussed above. The solvated particles are moved using the BD equation above with a time constant of  $1 \times 10^{-12}$  s. A particle is assumed to adsorb to the surface if, over the course of

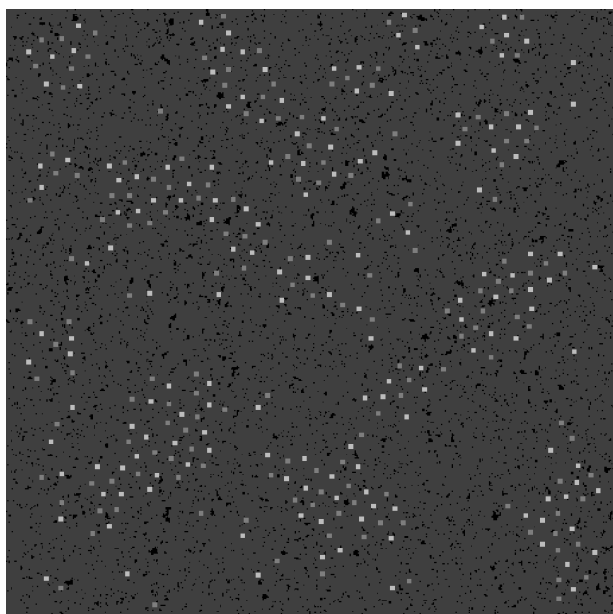


Figure 5. Results from  $150 \times 10^6$  Monte-Carlo steps of the 2D simulation with Coulombic and LJ interactions on a  $512 \times 52$  grid. The particles carry either a negative (light squares) or positive (dark gray squares) charge. The simulation parameters are:  $\epsilon_{LJ} = 8.2842 \times 10^{-21}$  J, and  $\kappa = 1.00 \times 10^7$  m. All other parameters not defined in the text are the same as in figure 2.

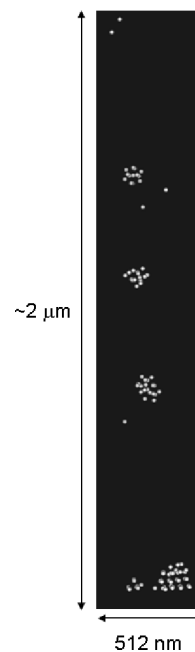


Figure 6. A snap shot of a system of 100 nanoparticles after 10  $\mu$ s of BD simulation and 50,000 Monte Carlo steps. The nanoparticles in the upper portion of the figure are in solution. The small set of spheres at the bottom that are all on the same plane are the adsorbed particles. The simulation parameters are:  $512 \times 512$  grid,  $\rho = 0.006$ ,  $\epsilon_l = 8.2842 \times 10^{-21}$  J,  $\epsilon_n = 1.65684 \times 10^{-20}$  J,  $\epsilon_{nl} = 1.24263 \times 10^{-20}$  J,  $\epsilon_{LJ} = 8.2842 \times 10^{-21}$  J and  $\kappa = 1.00 \times 10^7$  m.

the BD simulation, it comes within a particle-radius (2.0 nm in these simulations) of the surface. The particle movement is then controlled by the 2D-lattice simulation. The adsorbed particle is still allowed to interact with the other particles in the simulation through the LJ potential. To infer the loss of solvent due to evaporation in the BD simulation, the  $z$ -coordinate is reduced by 1.0 nm at equally spaced times throughout the simulation. The total distance change in this direction for these simulations is 100 nm. The multiscale simulation results presented in this paper have been run with 200 BD steps per lattice step. The surface particles are held constant during the energy calculations in the 200 BD steps, and the solvated particles are held constant during the energy calculations of 2D step. This simple approach allows for quick verification of the simulation procedures, and are reasonable, first-order approximations of the system.

Results from a simulation with 100 particles are shown in figures 6 and 7. The solvated particles have been confined to a cylinder that is  $2.0 \mu$ m tall and has a radius of 64.0 nm by re-randomizing the coordinates of the particle if it moves past the boundary. The value of  $\mu$  was made position dependent by using

$$\mu = k_B T \left( e^{\left(\frac{n}{n_0} - r\right)} - 4.5 \right), \quad (5)$$

where  $n$  was taken as the number of rows used in the 2D grid and  $r$  is the distance of a given grid cell from the center of the grid. This allows the solvent on the surface to dry faster at the edges than at the center. Further refinement of

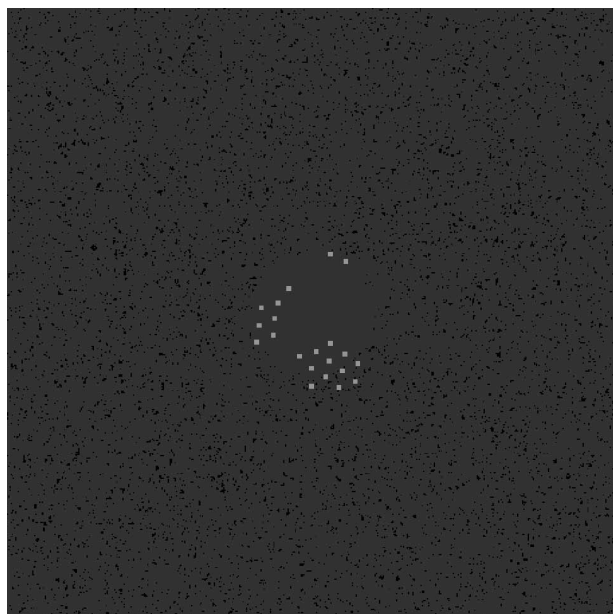


Figure 7. The results of 50,000 Monte Carlo steps of the BD-2D hybrid simulation. The particles adsorb as the BD simulation brings the particles to the surface. The 2D simulation allows the particles to move, and the surface solvent to evaporate. The light gray squares are the nanoparticles, the dark gray squares are the solvent, and the black areas are where the solvent has evaporated. The simulation parameters are the same as in figure 6.

the drying process is warranted, but it is obvious that these short simulations are not drastically altered by the steps taken to model the evaporation of the solvent. Further simulations of higher concentrations of nanoparticles over longer time scales will be used to determine the refinements necessary to model the deposition of the nanoparticles as the solvent dries.

Figure 6 shows that the nanoparticles group together into spheres while they are in solution. This is due to the LJ forces. At this point in the simulation, the particles have formed three groups in solution. The groups consist of 16 nanoparticles on average. The figure also shows the positions of the adsorbed nanoparticles. The motion of the adsorbed particles is modeled using the coarse-grained model discussed above. It is interesting to note that the adsorbed molecules are forming a closest-packed type structure within the plane of the surface as seen in figure 7. It is also easy to observe the effects of the radial dependence of  $\mu$  on the coarse-grained system. The solvent is evaporating from the edges of the system first. There is a region that remains covered in solvent. Future work will allow the radial dependence to be time dependent as well, allowing the boundary of the liquid edge to move as the simulation progresses through time.

#### 4. Summary

We have proposed a new hybrid simulation algorithm in order to study the adsorption and aggregation of particles

as they are deposited on a surface. Particle-particle interactions have been extended from nearest-neighbor interaction through the addition of LJ and electrostatic terms. Particle-solvent and particle-surface interactions are parameterized. We have been able to show that the algorithm leads to the coalescence of the particles; however, we have not observed any structuring beyond amorphous surface clusters. Our next study will vary the system parameters to test whether structuring of the nanoparticle aggregates can occur. We also plan to introduce a shape factor which appears to be important in reported experimental results.

#### Acknowledgements

The authors would like to acknowledge NEC for supplying computer equipment used in the development and implementation of the simulation, and funding support from the National Science Foundation (EEC-0234002, MRI-0321147, CHE-0416090), and the US Department of Education (P116Z040100, P116Z05033).

#### References

- [1] C. Loo, A. Lowery, N. Halas, J. West, R. Drezek. Immunotargeted nanoshells for integrated cancer imaging and therapy. *Nano. Lett.*, **5**(4), 709 (2005).
- [2] G. Reiss, A. Huetten. Magnetic nanoparticles: applications beyond data storage. *Nat. Mater.*, **4**(10), 725 (2005).
- [3] I.L. Medintz, H.T. Uyeda, E.R. Goldman, H. Mattoussi. Quantum dot bioconjugates for imaging, labeling and sensing. *Nat. Mater.*, **4**, 435 (2005).
- [4] T.M. Allen, P.R. Cullis. Drug delivery systems: entering the mainstream. *Science* (Washington, DC, United States) **303**(5665), 1818 (2004).
- [5] P. Alivisatos. The use of nanocrystals in biological detection. *Nat. Biotechnol.*, **22**, 47 (2004).
- [6] S.M. Liu, S. Sato, K. Kimura. Synthesis of luminescent silicon nanopowders redispersible to various solvents. *Langmuir*, **21**(14), 6324 (2005).
- [7] M.G. Sandros, D. Gao, D.E. Benson. A modular nanoparticle-based system for reagentless small molecule biosensing. *J. Am. Chem. Soc.*, **127**(35), 12198 (2005).
- [8] J. Won, M. Kim, Y.-W. Yi, Y.H. Kim, N. Jung, T.K. Kim. A magnetic nanoprobe technology for detecting molecular interactions in live cells. *Science*, (Washington, DC, United States) **309**(5731), 121 (2005).
- [9] T.K. Sau, C.J. Murphy. Self-assembly patterns formed upon solvent evaporation of aqueous cetyltrimethylammonium bromide-coated gold nanoparticles of various shapes. *Langmuir*, **21**(7), 2923 (2005).
- [10] V.V. Vysotskii, V.I. Roldughin, O.Ya. Uryupina. Formation of fractal structures upon the evaporation of nanoparticle dispersion droplets. *Colloid J.*, **66**(6), 777 (2004).
- [11] J.G. Pagan, M.T. Ahrens, E.B. Stokes, B.A. Martin, M.A. Hasan. Integration of cdse quantum dots with gan optoelectronic materials. *Phys. Status Solidi. C Conf. Crit. Rev.*, **2**(7), 2924 (2005).
- [12] S. Coe-Sullivan, J.S. Steckel, W.-K. Woo, M.G. Bawendi, V. Bulovic. Large-area ordered quantum-dot monolayers via phase separation during spin-casting. *Adv. Funct. Mater.*, **15**(7), 1117 (2005).
- [13] G.A. Buxton, A.C. Balazs. Predicting the mechanical and electrical properties of nanocomposites formed from polymer blends and nanorods. *Mol. Simul.*, **30**(4), 249 (2004).
- [14] M. Fujita, H. Nishikawa, T. Okubo, Y. Yamaguchi. Multiscale simulation of two-dimensional self-organization of nanoparticles in liquid film. *Jpn. J. Appl. Phys. Part 1*, **43**(7A), 4434 (2004).

- [15] J.J. Gray, R.T. Bonnecaze. Adsorption of charge-bidisperse mixtures of colloidal particles. *Langmuir*, **17**(25), 7935 (2001).
- [16] J.J. Gray, R.T. Bonnecaze. Adsorption of colloidal particles by Brownian dynamics simulation. Kinetics and surface structures. *J. Chem. Phys.*, **114**(3), 1366 (2001).
- [17] C. Neto, M. Bonini, P. Baglioni. Self-assembly of magnetic nanoparticles into complex superstructures: spokes and spirals. *Colloids Surf. A Physicochem. Eng. Asp.*, **269**(1–3), 96 (2005).
- [18] A. Malevanets, R. Kapral. Solute molecular dynamics in a mesoscale solvent. *J. Chem. Phys.*, **112**, 7260 (2000).
- [19] A. Chatterji, J. Horbach. Combining molecular dynamics with lattice Boltzmann: a hybrid method for the simulation of (charged) colloidal systems. *J. Chem. Phys.*, **122**, 184903 (2005).
- [20] I. Pagonabarraga, D. Frenkel. Dissipative particle dynamics for interacting systems. *J. Chem. Phys.*, **115**, 5015 (2001).
- [21] F. Jarai-Szabo, S. Astilean, Z. Neda. Understanding self-assembled nanosphere patterns. *Chem. Phys. Lett.*, **408**(4–6), 241 (2005).
- [22] E. Rabani, D.R. Reichman, P.L. Geissler, L.E. Brus. Drying-mediated self assembly of nanoparticle. *Nature*, **426**, 271 (2003).
- [23] C.G. Sztrum, O. Hod, E. Rabani. Self-assembly of nanoparticles in three-dimensions: formation of stalagmites. *J. Phys. Chem. B*, **109**(14), 6741 (2005).
- [24] C. McCabe, S.C. Glotzer, J. Kieffer, M. Neurock, P.T. Cummings. Multiscale simulation of the synthesis, assembly and properties of nanostructured organic/inorganic hybrid materials. *J. Comput. Theor. Nanosci.*, **1**(3), 265 (2004).
- [25] R.A. Robinson, R.H. Stokes. *Electrolyte Solutions*, chapter 4, pp. 78–79, Dover Publications, Inc., Mineola, New York (2002).
- [26] D.L. Ermak, J.A. McCammon. Brownian dynamics with hydrodynamic interactions. *J. Chem. Phys.*, **69**, 1352 (1978).